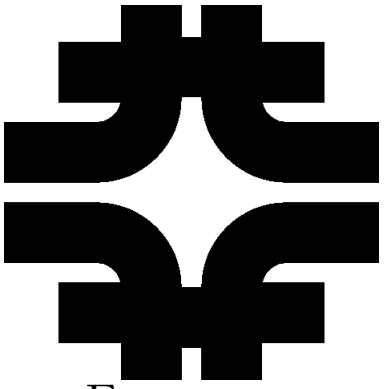

FERMILAB

PXIE

SSR1 Dressed Cavities

Author: Adam Carreon

Supervisor: Leonardo Ristori

August 7, 2012

Abstract

The SSR1 resonator is a superconducting single spoke resonator developed by Fermilab for the use in a future project called Project X. The following document outlines the Engineering Note that was created for the Dressed SSR1 resonator and also discusses analyses that were performed on the support arms of the tuner system on the SSR1 resonator. Much information was needed to be produced, gathered, and understood when creating the engineering note for the SSR1 resonator. The information needed was demanded by the ASME Boiler and Pressure Vessel Code by way of failure mode requirements that the SSR1 resonator's pressure vessels must meet. It took an effort of several people to bring together all of the information needed to produce the engineering note. After several weeks of CAD model testing the dressed SSR1 resonator proved to be a well designed vessel system by meeting all of the failure mode requirements given by the ASME Code.

The support arms is one of the several components the tuner system was broken down in to. By initially considering the tuning system as a whole, and having a stiffness goal, the stiffness of these several components where approximated. Using the approximated stiffness of the support arms and conceptual designs of the tuner system, an outline of the support arm shape was created. Several CAD model analyses were then performed to give a support arm design that meets stiffness and stress requirements.

1 Introduction

The SSR1 resonator is a superconducting single spoke resonator developed by Fermilab initially for the High Intensity Neutrino Source (HINS) accelerator. Similar SSR1 resonators will be used in a cryomodule for the Project X Injector Experiment (PXIE), which is the current research and development program for Project X. PXIE will make use of the SSR1 resonator in a continuous wave (CW) linac to justify the Project X experiment and to help gain experience with superconducting proton linear accelerators (linacs) [1]. Before the cryomodule can be fabricated some additional work, work done both to the cavity's engineering information note and to the cavity's tuner design, must be completed. The SSR1 resonator is composed of two pressure vessels and a tuning system. The engineering information note encompasses American Society of Mechanical Engineers (ASME) Boiler and Pressure Vessel (BPV) Code analyses dealing with the pressure vessels of the SSR1 resonator. The tuning system is an exterior addition to the SSR1 resonator and therefore has separate analyses and requirements.

The inner-most pressure vessel is the niobium (Nb) single spoke cavity. The niobium cavity is a superconducting cavity and has adopted a similar geometry to the one used for the HINS experiment. A computer aided design (CAD) model of the niobium cavity can be seen in Figure 1. Most of the shell, inner spoke, reinforcing ribs, and connecting ports are all machined from niobium. The several locations on this cavity that are not niobium include the connecting pipes at the beam pipes, vacuum port, and power coupler locations; the material chosen for their construction was stainless steel 316L (SS316L). SS316L was the material of choice because it is an ASME BPV Code material and because it is a non-magnetic material.

The outer-most pressure vessel is the SS316L helium vessel, and the main focus of the engineering note. The helium vessel surrounds the niobium cavity and contains the liquid helium bath when the cryomodule is operating at cryogenic temperatures. The helium vessel has been redesigned to meet the new requirements of PXIE [2]. In the HINS accelerator, the first generation SSR1, the pressure requirements set forward were strictly for safe operation in the cryomodule. PXIE, being a different experiment has different cavity requirements and thus, led to new generations of the helium vessel that would meet said requirements. These new requirements were mostly concerned with the $\frac{df}{dP}$ value of the helium vessel. The transition ring and newly curved shape of the third generation helium vessel addressed these issues. The helium vessel is designed to withhold liquid helium at a temperature of 2 K. The helium vessel also provides several support locations for the attachment of separate components. Two stand-like supports are welded to the shell of the helium vessel, holding the tuner horizontally, which are needed for installation in the cryomodule. Also, two bolting platforms are welded 180° from one another on the shell of the helium vessel which support the tuning system. Either pressure vessel, both shown below, must abide by the requirements given in one of the following manuals: Fermilab Environment, Safety, and Health Manual (FESHM) or the ASME BPV Code.

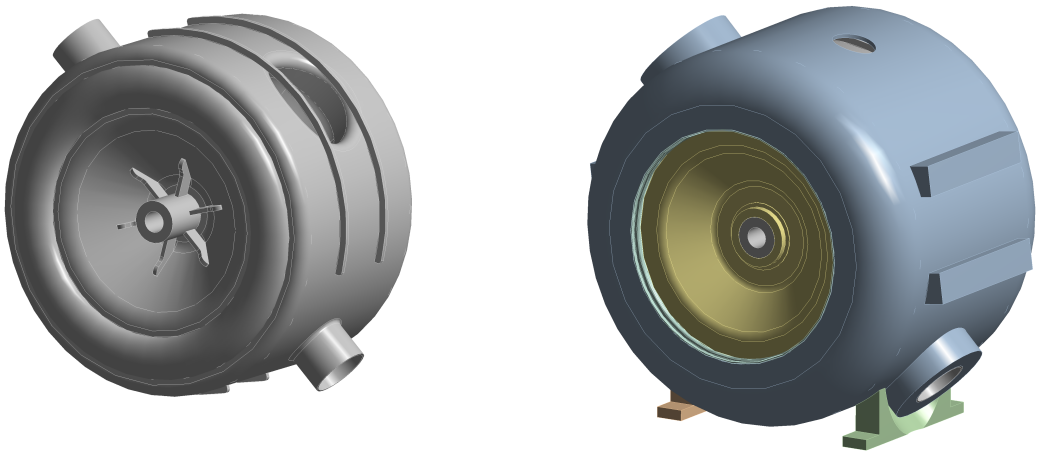

Figure 1: Shown above are views of both the niobium cavity (left) and the helium vessel (right) used in the failure mode analyses.

Shown here below is a labelled CAD model of the SSR1 resonator followed by component details:

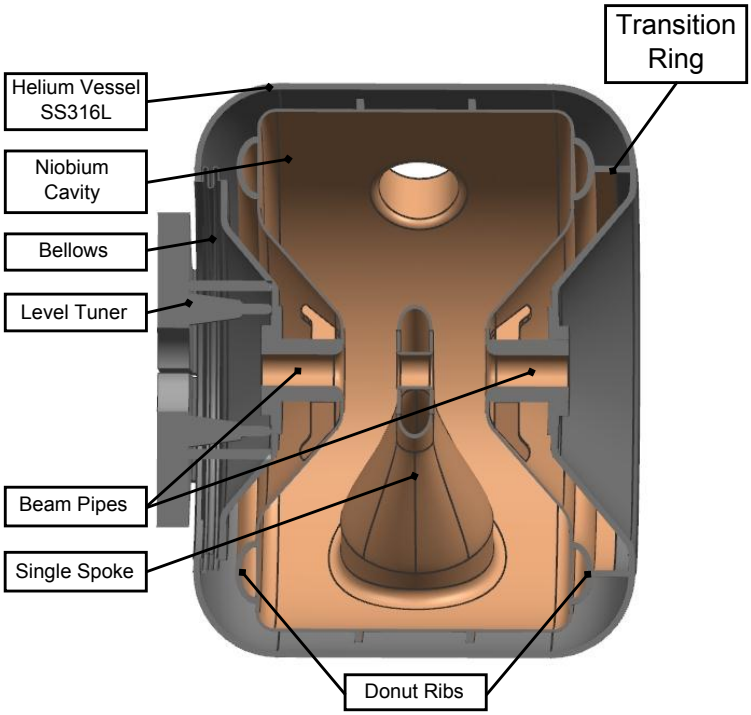

The annular space between the cylindrical shells of the pressure vessels is bridged by two service ports as well as a transition ring. These service ports are the vacuum and power coupler ports of the SSR1 resonator. The heads of the vessels are connected through a bellows, and attached to the bellows is the tuning system. Additional ports on the SSR1 resonator include the cryo connections. These connecting ports have stainless steel flanges that are furnace-brazed to the niobium cavity.

- **Bellows** - The purpose of the bellows in the SSR1 resonator is to utilize it's geometry to expand and contract under applied forces while not becoming plastically deformed. This characteristic enables the frequency of the SSR1 resonator to be tuned while operating.

- **Tuning System** - The tuning system deflects the bellows (helium vessel) such that the resonant frequency of the SSR1 resonator, 325 MHz, is always maintained during operation. To effectively accommodate for the frequency range and resolution of cavities, the tuner design includes both a coarse and fine tuning device engineered as one. [2]

- **Vacuum Pumpout Port** - The purpose of this port is to get the cavity to the desired pressure for the operation of the SSR1 resonator. For the analysis done on the SSR1 resonator, there were two pressures that were of interest. For room temperatures a Maximum Allowable Working Pressure ($MAWP_{RT}$) of no less than 2 bar was used. For cryogenic temperatures a Maximum Allowable Working Pressure ($MAWP_{CT}$) of no less than 4 bar was used.

- **Input Power Coupler** - The purpose of this port is to act as the connection between the coaxial coupler and the superconducting cavity. It is this input coupler that provides the electromagnetic power to the cavity. The coupler needs to transfer the power to the beam and the cavity field at a high power level.

- **Cryo Connections** - The purpose of this port it to connect the pipes that allow the helium bath to flow into the SSR1 resonator, ensuring that the vessels are at cryogenic temperatures when they need to be.

- **Transition Ring** - The purpose of the transition ring is to reduce the SSR1 resonator's sensitivity to fluctuations in helium pressure. This will allow the system to be more stable when it comes time maintain operation near the resonant frequency. This fluctuation is measured by calculating the $\frac{df}{dP}$ of the SSR1 resonator; where f is the instantaneous frequency and P is the corresponding pressure of the SSR1 resonator. The first generation SSR1 resonator, used in the HINS accelerator, had no restriction on this value and as a result had a high $\frac{df}{dP}$. Due to PXIE being a CW accelerator restrictions on this value have been imposed and generation three of the SSR1 resonator has a transition ring to reduce $\frac{df}{dP}$ to an acceptable value.

The tuning system as of the start of May 2012 was only a conceptual design developed from CAD models. This conceptual design gave an outline and placement on the SSR1 resonator of the tuning system. Starting in June, the tuning system has been undergoing re-design, optimization and analysis piece by piece. The system rendered grey in this CAD model is the conceptual tuning system; here the original designs are shown and how it will be attached to the helium vessel.

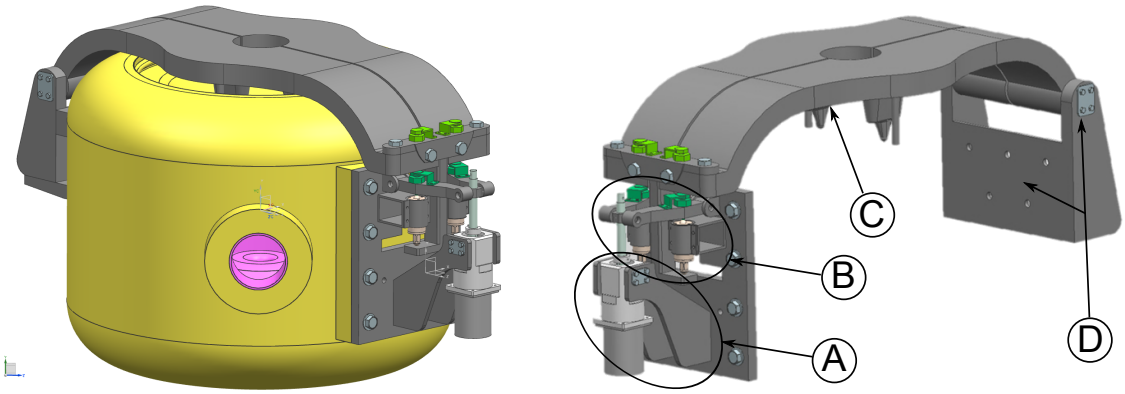

Figure 2: Shown above on the left is the complete SSR1 resonator. Shown on the right is the tuning system that is seen on the SSR1 resonator on the left.

There are four separate components the tuning system can be broken down into. Starting from the right of the tuner system, there is the connection to the helium vessel and tuner arm (D), the tuner arm (C), the fine/coarse piezoelectric/motor system (B), the support arm and bolted plate (A).

In this paper the support arms holding the coarse motor will be discussed. For the support arms, stiffness requirement value was given that needed to be met. This stiffness was approximated by measuring the allowable deflection of the tuner system as a whole, then assigning an appropriate allowable stiffness to each component. The bolted plate is one of the two connections of the tuner system to the helium vessel. The plate will need to be able to withstand the tensile and shear forces applied by the tuner motor, and do so with a minimal amount of deflection. Also, one important requirement is that the support-plate system have the ability to be removed from the helium vessel and cryomodule. This requires that the support arm and plate system be of small size in order to be removed from the cryomodule. This aspect of the SSR1 resonator is more theoretical than the pressure vessels and requires acquired course knowledge being applied with engineering experience to develop a working design.

The purpose of the engineering note analyses was to ensure that the dressed SSR1 SRF resonator complies to the ASME Boiler and Pressure Vessel Code [1], respecting the technical specifications which require a maximum allowable working pressure (MAWP) of 0.2 MPa (29 psi) at 293 K and 0.4 MPa (58 psi) at 2 K. The engineering note for the SSR1 resonator requires that several failure mode analyses are understood and performed to demonstrate that the SSR1 resonator meets the requirements set forth by the ASME BPV Code. Reading the ASME BPV Code, to understand what the required analyses are, was the initial step to forming the engineering note for the SSR1 resonator. Four failure modes analyses were performed on the SSR1 resonator and the details are discussed below in section 2. The tuner system is an important part of the SSR1 resonator when it comes to producing and maintaining precise deflections of the bellows. The component of the tuning system that will be discussed in this paper is the coarse motor support attached to the helium vessel. The main focus regarding the components of the tuning system was to design each of them such that the desired tuner displacement from the tuning force equalled the actual bellow displacement as accurately as possible.

2 Methods

2.1 Pressure Vessels

For pressure vessels, the ASME BPV Code sets forth the rules of safety for design and fabrication. The ASME BPV Code gives step-by-step instructions on how to properly execute each analysis as well as guidelines

regarding how to evaluate the results. Section VIII, Division 2, Part 5, of the ASME BPV Code provides the design-by-analysis requirements chosen to protect the SSR1 resonator against several different failure modes. The failure modes that apply to PXIE and the SSR1 resonator include, Protection Against Plastic Collapse, Protection Against Local Failure, Protection Against Collapse From Buckling, and Protection Against Failure From Cyclic Loading (Ratcheting). Multiple assessment procedures may be provided for a single failure mode; in this case only one procedure must be satisfied to qualify the design of a component.

The purpose of the design-by-analysis methodology is to achieve the desired Maximum Allowable Working Pressure (MAWP) which is defined for both working temperatures by the following:

- $MAWP_{RT} \geq 0.2\,MPa$ at Room Temperature (RT - $293K$)
- $MAWP_{CT} \geq 0.4\,MPa$ at Cryogenic Temperature (CT - $2K$)

The $MAWP$, for each temperature, was determined experimentally and distributed to appropriate teams to be used in their analyses. Two options arise when deciding upon how to use the given information; either the values are directly put into the analyses or used in a separate analysis to determine and compare a new $MAWP$ for each temperature. For the analyses of the engineering note the latter process was chosen, and the two $MAWP$s were determined using a separate simulation method; the $MAWP$s found through the analysis were then compared to the values determined experimentally (given). If these desired $MAWP$s are obtained while avoiding failure in all of the forms previously listed, then the SSR1 resonator has met the general requirements of the Code's Section VIII, Div. 2, Part 5.

To perform all of the analyses given by the ASME BPV Code, the following stress-strain curves of niobium and SS316L are needed:

- **Linear Elastic curve**: Presented below are both material properties that have been utilized in the linear elastic analyses performed. Throughout all the analyses it was assumed that the SS316L had consistent mechanical properties at all temperatures.

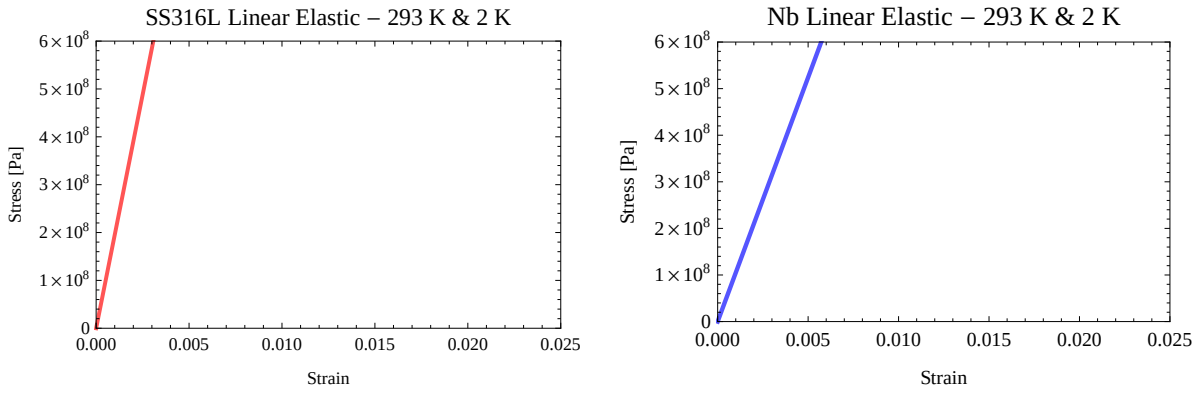

Figure 3: Shown above are the Linear Elastic Stress Strain curves for SS316L (left) and Nb (right) at both room temperature and cryogenic temperatures.

Table 1: Mechanical Properties of SS316L (ASME Code)

T $[K]$	E $[GPa]$	ν
2	195	0.3

Table 2: Mechanical Properties of Niobium (Nb)

T $[K]$	E $[GPa]$	ν
295.15	104.8	0.38
2	104.8	0.38

- **Linear Elastic-Perfectly Plastic curve**: Presented below are both material properties that have been utilized in the linear elastic-perfectly plastic analyses performed. Throughout all the analyses it was assumed that the SS316L had consistent mechanical properties at all temperatures.

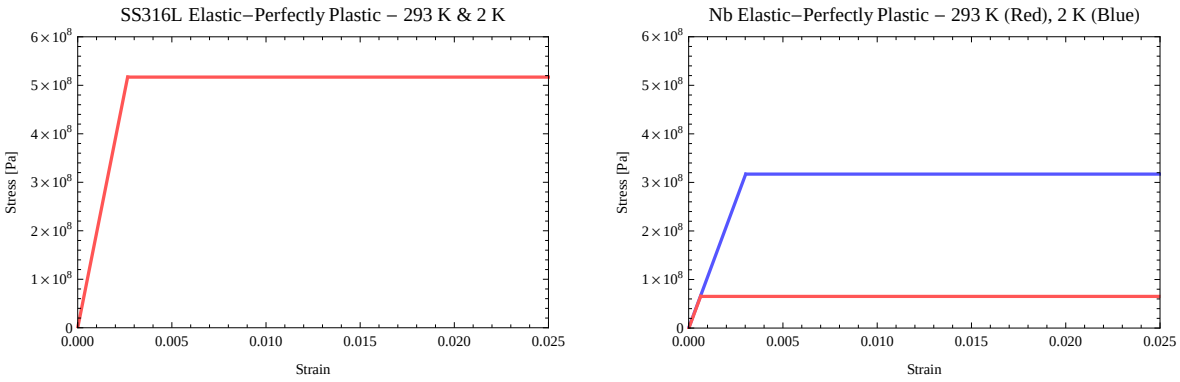

Figure 4: Shown above are the Elastic-Perfectly Plastic Stress Strain curves for SS316L (left) and Nb (right) at both room temperature and cryogenic temperatures.

Table 3: Mechanical Properties of SS316L (ASME Code)

T $[K]$	E $[GPa]$	ν	Y_s $[MPa]$
2	195	0.3	517

Table 4: Mechanical Properties of Niobium (Nb)

T $[K]$	E $[GPa]$	ν	Y_s $[MPa]$
295.15	104.8	0.38	75
2	104.8	0.38	317

- **Elastic-Plastic curve**: Presented below are both material properties that have been utilized in the elastic plastic analyses performed. Throughout all the analyses it was assumed that the SS316L had consistent mechanical properties at all temperatures.

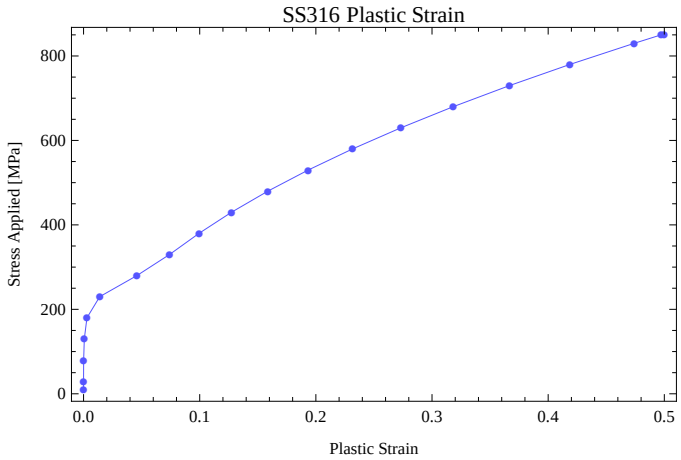

Figure 5: Plastic stress strain curve for SS316L

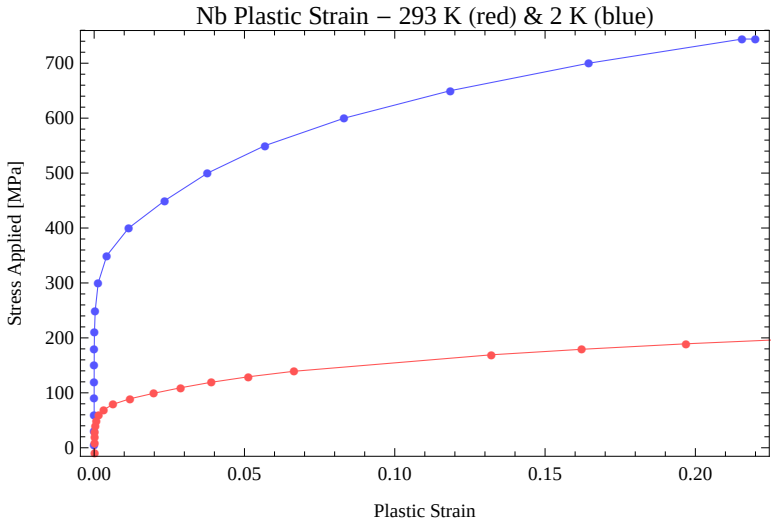

Figure 6: Shown above are the Plastic Stress Strain curves for Nb at room temperature (red) and cryogenic temperature (blue)

Table 5: Mechanical Properties of SS316L (ASME Code)

T $[K]$	E $[GPa]$	ν	Y_s $[MPa]$	Y_{ut} $[MPa]$	ε_p	m_2	R
2	195	0.3	517	172	$2.0 \cdot 10^{-5}$	$0.75(1.0 - R)$	3

Table 6: Mechanical Properties of Niobium (Nb)

T $[K]$	E $[GPa]$	ν	Y_s $[MPa]$	Y_{ut} $[MPa]$	ε_p	m_2	R
295.15	104.8	0.38	75	166	$2.0 \cdot 10^{-5}$	$0.5(0.98 - R)$	0.45
2	104.8	0.38	317	600	$2.0 \cdot 10^{-5}$	$0.5(0.98 - R)$	0.53

For either material, the Code did not contain information regarding integrated thermal contractions ranging from the temperatures of interest, $293\,K - 2\,K$. The FESHM was used for the thermal contraction value of niobium and [8] was used for SS316L.

Table 7: Coefficient of Thermal Contraction Values

α	Nb	SS316L
293 K	0	0
2 K	$5 \cdot 10^{-6}$	$1.013 \cdot 10^{-5}$

- **Protection Against Plastic Collapse**
  - *The analysis for this failure mode focuses on the internal pressure of the vessel and prevents plastic instability, ensuring that the pressure vessel does not experience plastic deformation that may lead to collapse. Also, the analysis avoids unbound displacement in each cross-section of the SSR1 resonator.*

Three separate methods are presented in the ASME BPV Code's Section VIII, Div. 2, Part 5 for protection against plastic collapse. Each test requires that the material have a certain stress-strain behavior when performing the analysis.

Elastic Stress Analysis Method - This method makes use of perfectly elastic material through the computation of stresses using an elastic analysis, then classified into categories, and then limited to allowable values that have been conservatively established such that a plastic collapse will not occur.

Limit Load Method - This method makes use of a material whose tangent modulus becomes zero once the yield limit has been reached.

Elastic-Plastic Stress Analysis Method - This method makes use of a more realistic stress-strain behavior of the material. The allowable load in this method is the load resulting from the design factors being applied to the collapse load. The collapse load is a direct result from the elastic-plastic analysis with consideration of both the applied loads as well as the deformation attributes.

In the analysis for the note the third approach, elastic-plastic stress analysis method, has been chosen as it provides a more accurate assessment of the protection against plastic collapse. The increase in accuracy results from the structural behavior of the component being more closely represented when using this method. Another reason why the accuracy is increased in this method is because the stress strain curve associated with the elastic plastic stress-strain curve describes the stress-strain relationship more realistically than the other two analysis methods listed above. Refer to Firgures 3 - 6 above, to compare stress-strain curves.

The plastic collapse of the component is evaluated using an elastic-plastic stress analysis. The allowable load on the component is established by applying a design factor to the calculated plastic collapse load. This type of analysis provides a more accurate assessment of the protection against plastic collapse of a component relative to the other two approaches because the actual structural behavior is more closely approximated. The elastic plastic material model should be incorporated and should also include the temperature dependent hardening behavior provided in the Code's Section VIII, Div. 2, Part 5, Appendix 3.D. The load cases to be considered are those listed in Table 9 (reproduction of Table 5.5 of the Code's Section VIII, Div. 2, Part 5) and the loads themselves are listed in Table 8 (reproduction of Table 5.5 of the ASME Code's Section VIII, Div. 2, Part 5).

Table 8: Loads acting on SSR1 resonator. Reproduction of Table 5.2 from Section VIII, Div. 2.

Design Load Parameter	Description
P	Internal and external maximum allowable working pressure
P_S	Static head from liquid of bulk materials (e.g. catalyst)
D	Dead weight of the vessel, contents, and appurtenances at the location of interest, including the following: Weight of vessel including internals, supports (e.g., skirts, lugs, saddles, and legs), and appurtenances (e.g., platforms, ladders, etc) Weight of vessel contents under operating and test conditions Refractory linings, insulation Static reaction from the weight of attached equipment, such as motors, machinery, other vessels, and piping
L	Appurtenance live loading Effects of fluid momentum, steady state transient
E	Earthquake loads (see ASCE 7 for the specific definition of the earthquake load, as applicable)
W	Wind loads
W_{pt}	Is the pressure test wind load case. The design wind speed for this case shall be specified by the Owner-User
S_s	Snow loads
T	Is the self-restraining load case (i.e., thermal loads, applied displacements). This load case does not typically affect the collapse load, but should be considered in cases where elastic follow-up causes stresses that do not relax sufficient to redistribute the load without excessive deformation.

Where, in the helium vessel engineering note analyses, the following loads apply:

- P - Pressure in the helium space under the fault condition
- P_S - Static head from liquid helium (considered as negligible)
- D - Dead weight of the vessel system
- T_1 - Applied tuner load of 7500 N
- T_2 - Cool-down from 293 K to 2 K

Where the pressure load will be applied normal to the annular red space shown in Figure 7, the tuner force will be applied normal to the beam pipe (along the arrows), the gravitational force applied to the center of mass (along yellow arrow), and the cooldown applied to the entire system.

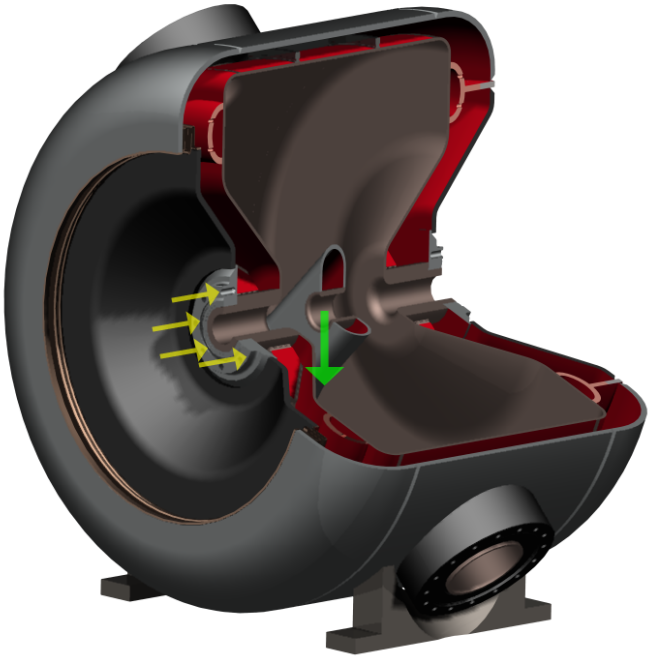

Figure 7: Shown here is the annular space where the helium pressure was applied (RED).

Table 9: Reproduction of used information in Table 5.5
Load Case Combinations and Load Factors for an Elastic-Plastic Analysis

Design Conditions	
Criteria	Required Factored Load Combinations
Global Criteria	1. $2.4(P + P_S + D)$ 2. $2.1(P + P_S + D + T) + 2.6L + 0.86S_S$
Local Criteria	$1.7(P + P_S + D)$

Specifically, in this analysis, the load cases considered are the following:

- Global Criterion 1: $2.4(P + D)$
- Global Criterion 2: $2.1(P + D + T_1 + T_2)$
- Global Criterion 2: $2.1(P + D + T_1)$

If convergence is achieved, the component is stable under the applied loads for the load case being considered. If convergence is not achieved and an error has occurred, then the component configuration shall be modified or applied loads reduced and the analysis repeated.

- **Protection Against Local Failure**
  - *The analysis for this failure mode focuses on the local strain limit for locations that have high stress values. It is a procedure to check and verify all the details of the SSR1 resonator (i.e. joints). This analysis ensures that the pressure vessel does not experience fracturing under the designed loads.*

The SSR1 resonator is multi-body system which has been brought together in multiple places by welds. All of the welds in the SSR1 resonator will be checked under the local failure criteria. There are three types of welds in the system that are to be analyzed. The welds under analysis are Tungsten Inert Gas (TIG) welds, brazed copper joints, and Electron Beam Welds (EBW). The cross-section shown below, Figure 8, of the SSR1 resonator gives the most complete view of the welds mentioned here.

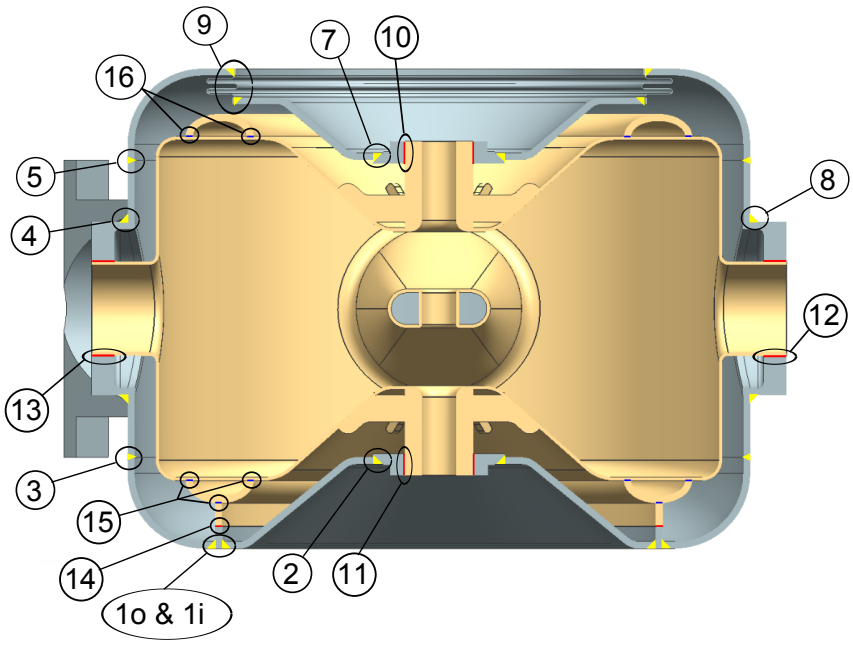

Figure 8: Shown above are views of both the helium vessel and the niobium cavity used in the analysis.

Table 10: Weld Descriptions of the welds labelled in Figure 8

Weld Number	Elements Joined	Weld Type	Weld Description
$1i$	HV to Transition Ring (Inner)	TIG	Full Penetration Butt Welds and Fillet Welds with weld angles of 45°
$1o$	HV to Transition Ring (Outer)		
2	Plate to Beam Pipe		
3	HV to Head		
4	HV to Vacuum Port		
5	HV to Head		
$6ss$	HV to HV (Support Side)		
$6w$	HV to HV (Weld)		
7	Plate to Beam Pipe		
8	HV to Coupler Port		
9	Plate to Bellows		
10	Plate to Cavity	BRAZE	Furnace-brazed joint between SS316L and Nb using oxygen-free electrolytic copper as the filler metal
11	Plate to Cavity		
12	Cavity to Coupler Port		
13	Cavity to Vacuum Port		
14	Cavity to Transition Ring		
15	Donut Rib to Transition Ring	EBW	Full Penetration single pass electron beam weld
16	Cavity to Donut Rib		

The use of TIG welds in the SSR1 resonator allows for high quality, clean welds. In the case of the helium vessel system, the TIG welds are used to join the SS316L components together. The welds seen in Figure 8 are examples of TIG welds and are used to join similar materials together. There are two categories of TIG welds that are used to join the SS316L components together; they are butt welds and fillet welds.

Butt welds are used on the SSR1 resonator in several locations where the material connections are parallel and have no over-lap. Within the butt weld category, groove welds and bevel welds have been chosen to use on the SSR1 resonator. The groove welds used have a groove angle of 45° and are full-penetration welds. The bevel welds used have a bevel angle of 45°, with respect to the vertical, and are full-penetration welds as well. Fillet welds are used on the SSR1 resonator when the need to join two pieces of SS316L that are at a 90° angle from one another. The throat thickness of the fillet welds used is $7.5\,mm$.

Brazing, in the SSR1 resonator, is used when there is a need to join SS316L and Niobium components. These joints will occur at the transition ring, beam pipes, vacuum port, and power coupler port locations. Oxygen-free electrolytic copper was used in joining the two materials by a furnace-brazed joint. The furnace-brazing was done in a vacuum and multiple tests were made on the components to ensure the design and strength of the joint are sturdy [7]. The testing began with a visual inspection to see if any of the filler material was evident on the outer surface of the joints. Then a Mass Spectrometer Leak Detection (MSLD) test was performed on the joints to ensure the integrity of the joints. $19.05\,mm$ widths of the brazed joint sections were cut and tension tested to experimentally calculate the ultimate strengths at both room temperature and cryogenic temperature. The results of [7] concluded the joint strengths to be independent of temperature and had an average ultimate strength of $80.5\,MPa$ for three joint designs. Figure 8 shows, in red, the locations of brazed-joints on the SSR1 resonator.

Discussed in [9], room temperature shear tests were performed on a similar braze joint to that in [7] having a $31.75\,mm$ niobium tube brazed to a $25.4\,mm$ thick stainless steel flange. Having a joint area of $683.86\,mm^2$ the test sample was able to allow $29.8\,kN$ of force without failure or plastic deformation. Plastic deformation occurs above $29.8\,kN$ and the test sample was able to allow $213\,kN$ of force without catastrophic joint failure.

The EBW is used in the SSR1 resonator for only several locations. The two places EBWs are used are on the transition ring and on the donut ribs. Similar to the TIG weld this weld is full penetration.

There are two methods of analysis provided by the Code's Section VIII, Div. 2, Paragraph 5.3.2, for the evaluation of protection against local failure to limit the potential for fracture under designed applied loads. Of the two methods the approach that was taken with the SSR1 resonator was to perform a linear elastic analysis. The evaluation of this analysis consists of calculating three linearized "membrane plus bending principal stress" models. The linearized stresses of the SSR1 resonator need to be evaluated using Stress Concentration Lines (SCL) placed in the regions of highest stress. These high-stress regions occur at abrupt changes in geometry as well as changes in material. More on SCL can be found in Annex 5.A, Div. 2 of the ASME Code. The following elastic analysis criterion needs to be satisfied for each point in the system:

$$(\sigma_{1L} + \sigma_{2L} + \sigma_{3L}) \leq 4S \tag{1}$$

Where S is the allowable stress. The way the allowable stresses were calculated in this document is in accordance with the ASME BVP Code's Section II, Part D, Appendix 1, Table 1-100.

$$S = min\Big[\frac{\sigma_{uts}}{3.5}, \frac{2}{3}\sigma_{ys}\Big] \tag{2}$$

The right hand side of Equation 1 has been through some discussion as whether or not the multiplication of the weld joint efficiency is needed. To avoid the issue, it has been decided to report the results as the following ratio:

$$\eta = \frac{\sum \sigma_L}{4S} < 1 \tag{3}$$

With a number less that one meaning that the stress in that specific location meets the local failure criterion. The table below gives the values used for the allowable stresses. The allowable stresses for

the brazed joints were taken from [4]. The allowable stress for the TIG weld at cryogenic temperatures was taken from [5]. This is the reference for SS316L at cryogenic temperatures. There are no cryogenic properties provided by the Code at 2 K. [1]

Table 11: Allowable Stresses

	S_{RT} [MPa]	S_{CT} [MPa]
TIG Weld (SS316L)	115	395[1]
Braze Joint	66	–
EB Weld (Nb)	48	171

- **Protection Against Collapse from Buckling**
  - *The analysis for this failure mode focuses on the compressive stress of the vessel. The failure is characterized by a sudden failure of a structural component subjected to a high compressive stress. A point of failure will occur where the actual compressive stress is greater than the ultimate compressive stress the material can withstand.*

A design factor for protection against collapse from buckling shall be satisfied to avoid buckling of the SSR1 resonator with a compressive stress field under applied design loads. The design factor is based on the type of buckling analysis performed. The design factors shall be the minimum values used with the shell components of the SSR1 resonator when buckling loads are determined using a numerical solution. The following are the three types of buckling analysis:

1. **Type 1** - If the use of a bifurcation buckling analysis that has an elastic stress analysis without geometric non-linearities in the solution to determine the pre stress in the component, then a minimum design factor shall be used. This design factor is,

$$\boldsymbol{\Phi_B = \frac{2}{\beta_{cr}}} \tag{4}$$

   (Paragraph 5.4.1.3). The loading combination to use for the pre-stress analysis is given in Table 12. (reproduction of Table 5.3 of the Code's Section VIII, Div. 2, Part 5)

2. **Type 2** - If the use of a bifurcation buckling analysis that has an elastic-plastic stress analysis with the effects of non-linear geometry in the solution to determine the pre stress in the component, then a minimum design factor shall be used. This design factor is,

$$\boldsymbol{\Phi_B = \frac{1.667}{\beta_{cr}}} \tag{5}$$

   (Paragraph 5.4.1.3). The loading combination to use for the pre-stress analysis is given in Table 12. (reproduction of Table 5.3 of the Code's Section VIII, Div. 2, Part 5)

3. **Type 3** - If a collapse analysis is performed and imperfections are explicitly considered in the analysis model geometry, then the design factor is accounted for in the load combinations in Table 9 (reproduction of Table 5.5 of the Code's Section VIII, Div. 2 Part 5). This type of analysis can be done using either elastic or plastic behavior.

[1] This value was not provided by the Code, and was found according to [5]

Table 12: Reproduction of used information in Table 5.3

Load Case Combinations and Allowable Stresses for an Elastic Analysis	
Design Load Combination	Allowable Stress
1. $P + P_S + D$ 2. $P + P_S + D + L$ 3. $P + P_S + D + L + T$	• Determined based on the Stress Category shown in Figure 5.1

A Type 1 analysis has been the analysis chosen to perform on the system.

- **Protection Against Failure from Cyclic Loading**
  - *The analysis for this failure mode focuses on vessel components that experience a cyclic operation. The purpose of this analysis is to make an evaluation for fatigue based on the number of cycles the vessel will experience.*

To evaluate protection against ratcheting using elastic-plastic analysis, an assessment is performed by application, removal and re-application of the applied loadings. If protection against ratcheting is satisfied, it may be assumed that progression of the stress-strain hysteresis loop along the strain axis cannot be sustained with cycles and that the hysteresis loop will stabilize [1].

The following is the assessment procedure for the elastic-plastic stress ratcheting analysis:

- **STEP 1** - Develop a numerical model that accurately represents the SSR1 resonator geometry, boundary conditions, and applied loads.
- **STEP 2** - Define all relevant loads and applicable load cases from Table 5.1 (Figure 22)
- **STEP 3** - An elastic-perfectly plastic material model will need to be used in the analysis. The von Mises yield function and associated flow rule should be utilized. The yield strength defining the plastic limit shall be the minimum specified yield strength at temperature from Annex 3.D. Also, the effects of non-linear geometry will need to be considered in the analysis as well.
- **STEP 4** - Perform an elastic-perfectly plastic analysis for the applicable loading from STEP 2 for a number of repetitions of a loading event. The number of repetitions for a loading event can be determined by seeing Annex 5.B.
- **STEP 5** - Below are the ratcheting criteria that will be under evaluation after the application of a minimum of three complete repetitions of the cycle. Additional cycles my need to be applied to demonstrate convergence. If any one of the following condition are met, then the ratcheting criteria are satisfied
  1. There is no plastic action (plastic strain is zero) in the SSR1 resonator.
  2. There is an elastic core in the primary-load-bearing boundary of the SSR1 resonator.
  3. There is no plastic deformation in the overall dimensions of the SSR1 resonator. This can be demonstrated by developing a plot of relevant component dimensions versus time between the last and the next to the last cycles.

However, even though the cyclic analysis is mandatory, the ASME BPV Code gives a fatigue assessment which can be performed to tell whether or not the additional ratcheting analysis is necessary.

The following is the procedure for the Fatigue Analysis Screening, Method A:

- **STEP 1** - Determine a load history based on the information in the User's Design Specification. The load history should include all cyclic operating loads and events that are applied to the system. According to the system analysis that will be running for this system, there will only be three loads in the load history. They are the following:

    1. **STEP 2** - $N_{\Delta FP}$ - The expected number of full-range pressure cycles including startup and shutdown.
    2. **STEP 3** - $N_{\Delta PO}$ - The expected number of operating pressure cycles in which the range of pressure variation exceeds 20% of the design pressure for integral construction or 15% of the design pressure for non-integral construction. Pressure cycles in which the pressure variation does not exceed these percentages of the design pressure and pressure cycles caused by fluctuations in atmospheric conditions do not need to be considered in this evaluation.
    3. **STEP 4** - $N_{\Delta TE}$ - The effective number of changes in metal temperature difference between any two adjacent points, ΔT_E, as defined below:
        - Points are considered to be adjacent if they are within a distance L of each other.
            * For shells and dished heads in the meridional or circumferential directions,

            $$L = 2.5\sqrt{Rt} \tag{6}$$

            where R = inside radius measured normal to the surface from the mid-wall of the shell to the axis of revolution.
            * For flat plates,

            $$L = 3.5a \tag{7}$$

            where a = radius of hot spot or heated area within a plate or the depth of a flaw at a weld toe.
        - For through-the-thickness temperature differences, adjacent points are defined as any two points on a line normal to any surface on the component.

        The effective number of such changes is determined by multiplying the number of changes in metal temperature difference of a certain magnitude by the factor given in Table 5.8 (Figure 23), and then by adding the resulting numbers.
    4. **STEP 5** - $N_{\Delta T\alpha}$ - The number of temperature cycles for components involving welds between materials having different coefficients of thermal expansion that causes the value of $(\alpha_1 + \alpha_2)\Delta T$ to exceed 0.00034.

- **STEP 6** - If the expected number of operating cycles from STEPS 2, 3, 4, and 5 satisfy the criterion in Table 5.9 (Figure 24), then a fatigue analysis is not required as a part of the vessel design.

An additional load, $N_{\Delta Tuner}$, will need to be applied due to there being no direct analog among the cycle definitions. This value will then be added to the conditional equation from Table 5.9 (Figure 24).

For the Niobium cavity, the construction is integral.

- **Integral Construction** - Construction technique that supports structural load by using an object's external skin, as opposed to using an internal frame.

Also, there are neither attachments nor nozzles in the knuckle region of the formed heads. Therefore, the conditional equation used for this analysis will be the following:

$$N_{\Delta FP} + N_{\Delta PO} + N_{\Delta TE} + N_{\Delta T\alpha} + N_{\Delta Tuner} \leq 1000 \tag{8}$$

2.2 Tuner

The application of a tuner system to a resonator does not have a code to follow like what pressure vessels have. The design of the tuner system follows a theoretical approach. Therefore, the design guidelines for a tuning system must be addressed by engineers as to ensure that the system will operate efficiently and not fail under operating conditions. The focus for the coarse motor support arms is to get the stiffness of the support arms system close to $100,000 \frac{N}{mm}$. This specific value was set as the requirement value because a support less stiff than this value will have too much deflection and a support stiffer than this value will be unnecessary; in addition, another component of the SSR1 resonator will fail before the support arms do, provided the stiffness of the support arms are greater than $70,000 \frac{N}{mm}$. By designing the support arms for a stiffness of $100,000 \frac{N}{mm}$ a safety factor will be designed into this component of the tuning system.

The design process of the support arms began by observing the surrounding parameters that have been set forth previously in the conceptual CAD model of the tuning system. The distance the coarse motor is from the plate and the surrounding component placements were two set parameters that shaped the design of the support arms. To get an initial idea of what the dimensions of the beam should be, the support arms were simplified down to a beam shape to allow the use of simple mechanical beam equations. The following beam equation was chosen as the equation which represented the support arm system.

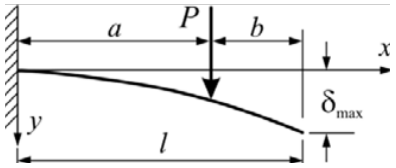

$$\delta_{max} = \frac{Pa^2}{6EI}(3l - a)$$

Figure 9: Shown above is the beam load (left) used to represent the support arm as well as the maximum deflection of the loaded beam (right) that represents the load case.

Since the above equation describes a beam the design of the support arm was developed to resemble a beam as closely as possible. There were several factors that altered the design of the support arms from that of a beam, such as the T-bar and the coarse motor sleeve. An outline of the design can be seen below:

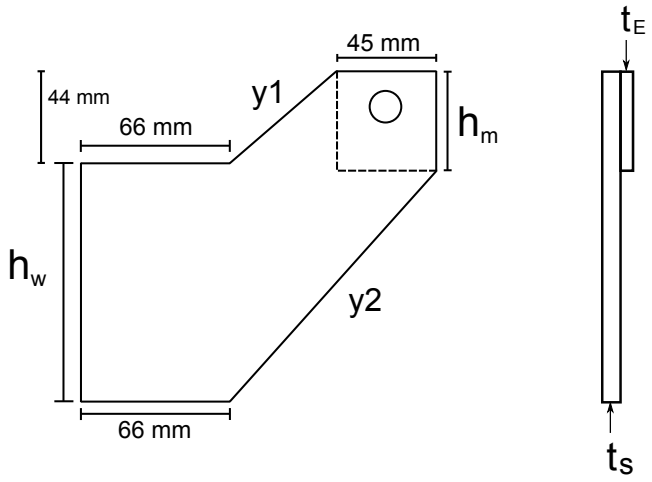

- h_w - This value is the height dimension of the end of the support beam attached to the plate.

- h_m - This value is the height dimension of the end of the support beam attached to the coarse motor. This is also the height of the extrusion near the coarse motor.
- $y1$ - This value is an equation that represents the top sloped line of the support arm. This equation is in a mathematical program developed to calculate the moment of inertia of the support arm given values of h_w and h_m.
- $y2$ - This value is an equation that represents the bottom sloped line of the support arm. This equation is in a mathematical program developed to calculate the moment of inertia of the support arm given values of h_w and h_m.
- t_E - This value is the extrusion thickness that occurs near the coarse motor.
- t_s - This value is the support arm thickness.

Using the surrounding tuner-component dimensions from the concept CAD model, approximated parameters of the support arms, and the known material properties of SS316L, the above deflection equation was used to calculate the needed moment of inertia of the approximated support beam. This moment of inertia was then set equal to the formula for the moment of inertia of a rectangle about its neutral axis. An initial thickness, t_s, was selected to get the moment of inertia. The extrusion thickness, t_E, only covered a small portion of the support arm and was therefore left out of the moment of inertia calculation. The dimensions of the support arm model that was used were the following; $h_w = 96\,mm$, $h_m = 45\,mm$, $t_s = 9\,mm$, and $t_E = 2\,mm$. There is also an additional $2\,mm$ wide and $2\,mm$ thick ring extrusion from the support arm pin hole added in the mathematical model.

The analysis for the support arms requires an FEA (Finite Element Analysis) that resembles the physical operation of the tuner system as accurately as possible. The purpose of this FEA is to determine the stiffness of the support arms. The stress will also be calculated, although it is known that the stress of this component will not be an issue. The model must then demonstrate that the support arm design can withstand the allowable stress given by the designed loads while having a stiffness near $100,000\,\frac{N}{mm}$. There will be three different phases in which the analysis will be set up, and as a result there will be three different stiffness values that will be obtained.

The first stiffness value that will be obtained is the easiest of the three to calculate and will give the support arm stiffness only. This stiffness value was estimated to have the middle stiffness value of the three. The second stiffness value introduces the coarse motor casing, bearings, and pin connections to the support arms. These added components will increase the stiffness of the system slightly giving a greater stiffness value than the support arm alone. The third stiffness value analysis requires the pressure vessels of the SSR1 resonator be included in the analysis. This calculated stiffness value is considered the "true" stiffness and requires a more complex model analysis. The "true" stiffness will be the smallest stiffness value calculated and therefore the support arm itself will be designed to a stiffness value greater than $100,000\,\frac{N}{mm}$. When creating the mathematical model for the "true" stiffness analysis the physical behavior the components should follow was found difficult to simulate accurately in the mathematical model. Therefore, a few approximate conditions were made in the model. Manual Spot Welding rings as screws, Manual Spot Welding bearing to motor, and having a rigid Planar interface between the plate and helium vessel were most of the approximations made in the final mathematical model.

3 Results

3.1 Pressure Vessels

3.1.1 Elastic Plastic Analysis for Protection Against Plastic Collapse

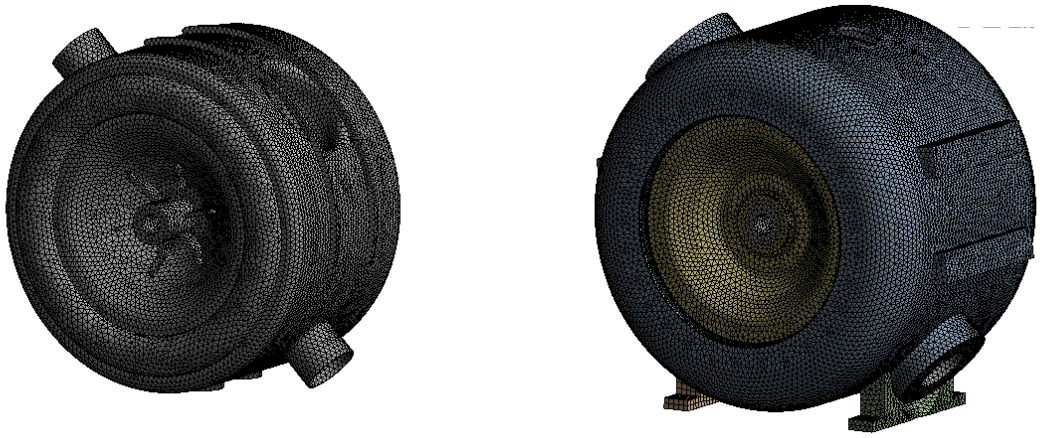

Figure 10: Shown above are views of both the helium-vessel-mesh and the niobium-cavity-mesh used in the Protection Against Plastic Collapse Analysis.

3.1.2 Global Criterion 1: RT Analysis

- **Loads** - The load combination in this analysis was the following:

$$2.4(P + D) \tag{9}$$

The loads were applied in the following two steps:

STEP 1 - Ramped Dead weight of the system (D). (Range time: 0 - 1 second)

STEP 2 - Constant Dead weight of the system (D) plus ramped Pressure (P) [$(0.8\,MPa)$]. (Range time: 1 - 2 seconds). The maximum pressure value chosen here is such that plastic collapse must occur within the created interval, $0 - 0.8\,MPa$.

The time of last solution evaluated was 1.841 *seconds*. This means that the MAWP at RT is:

$$MAWP_{RT} = \frac{0.8 \cdot 0.841}{2.4} = \frac{0.673}{2.4} = 0.280\,MPa\,(40.66\,psi) \tag{10}$$

3.1.3 Global Criterion 2: CT Analysis

- **Loads** - The load combination in this analysis was the following:

$$2.1(P + D + T_1 + T_2) \tag{11}$$

The loads were applied in the following two steps:

STEP 1 - Ramped Dead weight of the system (D) plus ramped Thermal cooldown to 2 K (T_2). (Range time: 0 - 1 seconds)

STEP 2 - Constant Dead weight of the system (D) plus ramped Pressure (P) [($2\ MPa$)]. (Range time: 1 - 2 seconds)

The time of last solution evaluated was 1.94226 *seconds* This means that the MAWP at CT is:

$$MAWP_{CT} = \frac{2 \cdot 0.94226}{2.1} = \frac{1.8845}{2.1} = 0.897\ MPa\ (130.1\ psi) \tag{12}$$

3.1.4 Global Criterion 2: RT Analysis

- **Loads** - The load combination in this analysis was the following:

$$2.1(P + D + T_1) \tag{13}$$

The loads were applied in the following two steps:

STEP 1 - Ramped Dead weight of the system (D) plus ramped Tuner system forces (T_1). (Range time: 0 - 1 second)

STEP 2 - Constant Dead weight of the system (D) plus ramped Pressure (P) [($0.8MPa$)]. (Range time: 1 - 2 seconds)

- **Results** - The time of last solution evaluated was 1.731 *seconds*. This gives a MAWP at RT of:

$$MAWP_{RT}^{GC2} = \frac{0.8 \cdot 0.731}{2.1} = \frac{0.585}{2.1} = 0.278\ MPa\ (40.3\ psi) \tag{14}$$

Figure 11 shows the region of plastic collapse.

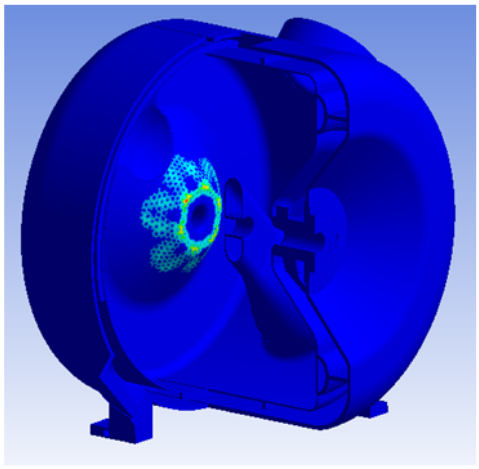

Figure 11: Shown here is the region of plastic collapse occurring near the daisy ribs.

3.1.5 Protection Against Collapse from Buckling

Figure 12: Shown above are views of both the helium-vessel-mesh and the niobium-cavity-mesh used in the Protection Against Buckling Analysis.

3.1.6 Buckling Analysis Type 1 - Room Temperature

- **Loads** - The load combination applied in this analysis was the following:

$$(P + D) \tag{15}$$

P = Helium Pressure [$MAWP_{RT}$ (0.2 MPa)]
D = Dead Weight of the System

Given the buckling pressure and the design factor, the Maximum Allowable Working Pressure at room temperature is,

$$MAWP_{RT} = \frac{3.309}{2.5} = 1.324\,MPa\,(192.36\,psi) \tag{16}$$

Figure 13 shows the 1^{st} buckling shape of the cavity at RT.

3.1.7 Buckling Analysis Type 1 - Cryogenic Temperature

- **Loads** - The load combination applied in this analysis was the following:

$$(P + D + T_2) \tag{17}$$

The loads were applied in the following two steps:

STEP 1 - Ramped Dead weight of the system (D) plus ramped Thermal cooldown to 2 K (T_2). (Range time: 0 - 1 second)

STEP 2 - Constant Dead weight of the system (D) plus ramped Pressure (P) [$(0.4\,MPa)$]. (Range time: 1 - 2 seconds)

Given the buckling pressure and the design factor, the Maximum Allowable Working Pressure at cryogenic temperature is,

$$MAWP_{CT} = \frac{2.793}{2.5} = 1.117\,MPa\,(162.04\,psi) \tag{18}$$

Figure 13 shows the 1^{st} buckling shape of the cavity at CT.

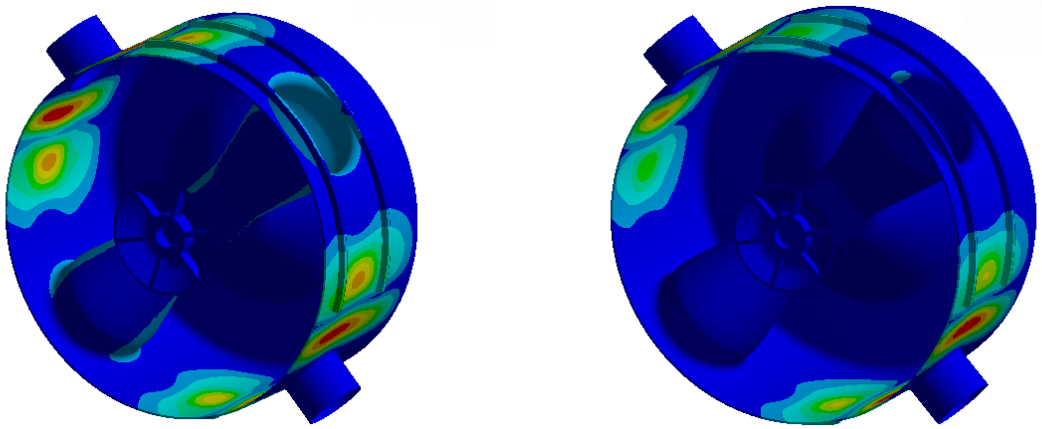

Figure 13: Shown above are views of the niobium cavity's first buckling shape in the buckling analysis at both RT (left) and CT (right).

3.1.8 Protection Against Failure from Cyclic Loading - Ratcheting

3.1.9 Ratcheting Analysis

- **Loads** - The cycle of loads taken into account for checking the protection against ratcheting had the following steps:

  STEP 1 - Ramped pressure in the helium space up to 0.2 MPa

  STEP 2 - Keeping the load from STEP 1 constant, apply thermal cooldown from 293 K to 2 K

  STEP 3 - Keeping the loads from STEPS 1-2 constant, apply ramped tuner force up to 7500 N

  STEP 4 - Keeping the loads from STEPS 2-3 constant, increase the pressure inside the helium space to 0.4 MPa

  STEP 5 - Keeping the loads from STEPS 2-3 constant, reduce the pressure inside the helium space to 0.2 MPa

  STEP 6 - Keeping the loads from STEPS 2 & 5, remove the tuner force applied at STEP 3

  STEP 7 - Keeping the load from STEP 5, remove the thermal cooldown (STEP 2) to return the system to 293 K

  STEP 8 - The end STEP; remove the last load still being applied, STEP 5, making the pressure inside the helium space equal to zero.

  – STEPS 1 - 4 develop the loading process in the system, while STEPS 5 - 8 develop the unloading process. Five complete repetitions of the cycle, STEPS 1 - 8, have been applied to the system to demonstrate convergence.

- **Results** - By creating a plot of relevant component dimensions versus time between CYCLE 4 and CYCLE 5, it has been demonstrated that there is no plastic deformation in the overall dimensions of the SSR1 resonator system. Therefore, with negligible changing of plastic deformation between the last two cycles the ratcheting criteria is satisfied.

Figure 7 shows the location and direction of displacement (location: beam pipe at end of yellow arrows, direction: yellow arrows) that the tuner applies to the beam pipe. The displacement value is 0.25 mm and occurs only during the cool-down phase.

3.1.10 Fatigue Assessment

- Following [3] an estimate of 200 has been given to $N_{\Delta FP}$.
- There will be no operation of an SSR1 resonator at a pressure deviating 20% from the design pressure.
- Following [3] an estimate of 100 has been given to $N_{\Delta TE}$.
- Following the temperature cycles used above in $N_{\Delta TE}$, an estimate of 100 has been given to $N_{\Delta T\alpha}$.
- Following [3] an estimate of 200 will be given to $N_{\Delta Tuner}$.

Estimates for the number of cycles of each loading type a cavity will need to withstand are given in the table below:

Table 13: Estimated Load History of SSR1 Resonator

Loading	Designation	Number of Cycles
Pressurization	$N_{\Delta FP}$	200
Cooldown	$N_{\Delta TE}$	100
Expansion	$N_{\Delta T\alpha}$	100
Tuning	$N_{\Delta Tuner}$	200

$$200 + 100 + 100 + 200 = 600 \leq 1000 \tag{19}$$

From the above equation it can be seen that the fatigue assessment criterion was satisfied, and therefore no fatigue analysis is necessary for the SSR1 resonator.

3.1.11 Protection Against Local Failure - Division 2

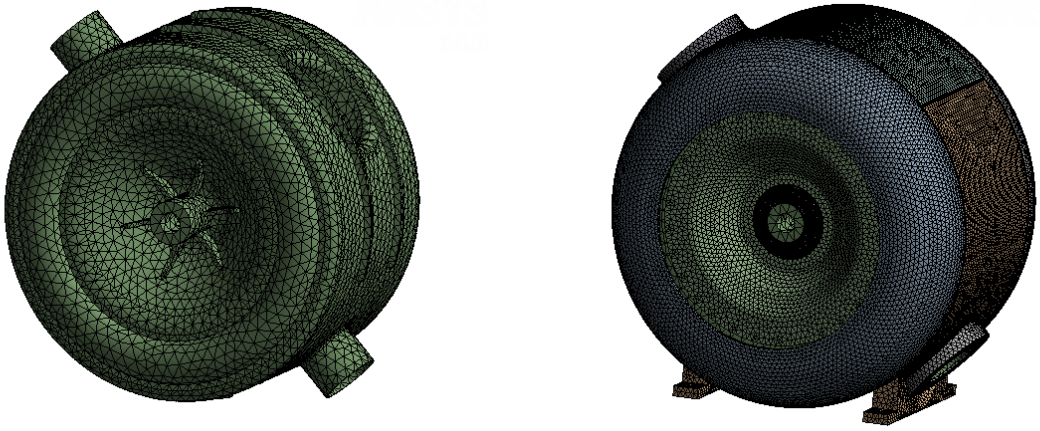

Figure 14: Shown above are views of both the helium-vessel-mesh and the niobium-cavity-mesh used in the Protection Against Local Failure Analysis.

3.1.12 Load Case 1: Room Temperature (NO Tuner Load)

Here the load case combination being analysed occurs at room temperature and can be found in Table 12 (reproduction of Table 5.3 in Div. 2 Part 5). The RT analysis will be divided into two load combinations. One load combination will include the load of the tuner, T_1, and the other will not.

- **Loads** - The load combination for this analysis was the following:

$$(P + D) \tag{20}$$

  $P = 0.2$ MPa (Helium Pressure) which is the target value for $MAWP_{RT}$
  $D =$ (mass of system)·(gravity)

- **Results** - The Principal Membrane + Bending (linearized) stress have been calculated through proper stress characterization lines (SCL) as stated by the ASME Code.

Table 14: Local Failure for Load Case 1 without Tuner Load

Weld Number Figure 8	Weld Location	Weld Type	$\sigma_{1L} + \sigma_{2L} + \sigma_{3L}$ [MPa]	η
7	BP Bellow Side	TIG	159.65	0.347
2	BP Ring Side	TIG	105.98	0.230
$1i$	Transition Ring Inside	TIG	38.95	0.085
$1o$	Transition Ring Outside	TIG	25.32	0.055
5	Cfr Bellow Side	TIG	11.94	0.026
3	Cfr Transition Ring Side	TIG	6.03	0.013
$6ss$	Longitudinal Support Side (NS)	TIG	17.03	0.037
$6w$	Longitudinal Weld (NS)	TIG	13.89	0.03
8	Vacuum Port	TIG	82.7	0.18
4	Power Coupler Port	TIG	81.27	0.177
11	BP Ring Side	$Braze$	58.9	0.223
10	BP Bellow Side	$Braze$	142.84	0.54
13	Power Coupler Port	$Braze$	26.68	0.056
12	Vacuum Port	$Braze$	14.91	0.10
14	Transition Ring SS316L	$Braze$	5.2	0.02
16	Donut Rib	EBW	38.49	0.2
15	Nb Transition Ring	EBW	40.7	0.21

3.1.13 Load Case 1: Room Temperature (Tuner Load)

- **Loads** - The load combination for this analysis was the following:

$$(P + D + T_1) \tag{21}$$

$P = 0.2$ MPa (Helium Pressure) which is the target value for $MAWP_{RT}$
$D =$ (mass of system)·(gravity)
$T_1 = 7500\ N$

- **Results** - The Principal Membrane + Bending (linearized) stress have been calculated through proper stress characterization lines (SCL) as stated by the ASME Code.

Table 15: Local Failure for Load Case 1 with Tuner Load

Weld Number Figure 8	Weld Location	Weld Type	$\sigma_{1L} + \sigma_{2L} + \sigma_{3L}$ [MPa]	η
7	BP Bellow Side	TIG	179	0.39
2	BP Ring Side	TIG	118	0.26
$1i$	Transition Ring Inside	TIG	45	0.1
$1o$	Transition Ring Outside	TIG	32	0.07
5	Cfr Bellow Side	TIG	14	0.03
3	Cfr Transition Ring Side	TIG	10	0.02
$6ss$	Longitudinal Support Side (NS)	TIG	41	0.09
$6w$	Longitudinal Weld (NS)	TIG	28	0.06
8	Vacuum Port	TIG	86	0.19
4	Power Coupler Port	TIG	110	0.24
10	BP Bellow Side	$Braze$	89	0.34
11	BP Ring Side	$Braze$	58	0.22
12	Vacuum Port	$Braze$	17	0.06
13	Power Coupler Port	$Braze$	16	0.06
14	Transition Ring SS316L	$Braze$	3.6	0.014
16	Donut Rib	EBW	40.717	0.21
15	Nb Transition Ring	EBW	44.33	0.23

3.1.14 Load Case 2: Cryogenic Temperature (NO Tuner Load)

Here we have the load case combination that occurs at cryogenic temperatures from Table 12 (reproduction of Table 5.3 from Div. 2 Part 5). As in the RT analysis, the CT analysis will be divided into two load combinations.

- **Loads** - The load combination for this analysis was the following:

$$(P + D + T_2) \tag{22}$$

$P = 0.4$ MPa (Helium Pressure) which is the target value for $MAWP_{CT}$
$D =$ (mass of system)·(gravity)
$T_2 =$ Loads due to thermal contraction

- **Results** - The Principal Membrane + Bending (linearized) stress have been calculated through proper stress characterization lines (SCL) as stated by the ASME Code.

Table 16: Local Failure for Load Case 2 without Tuner Load

Weld Number Figure 8	Weld Location	Weld Type	$\sigma_{1L} + \sigma_{2L} + \sigma_{3L}$ [MPa]	η
7	BP Bellow Side	TIG	319.2	0.2
2	BP Ring Side	TIG	158.83	0.1
$1i$	Transition Ring Inside	TIG	100.39	0.06
$1o$	Transition Ring Outside	TIG	64.65	0.04
5	Cfr Bellow Side	TIG	24.32	0.02
3	Cfr Transition Ring Side	TIG	16.54	0.01
$6ss$	Longitudinal Support Side (NS)	TIG	34.6	0.02
$6w$	Longitudinal Weld (NS)	TIG	26.36	0.02
8	Vacuum Port	TIG	165.51	0.1
4	Power Coupler Port	TIG	164.41	0.1
11	BP Ring Side	$Braze$	162	0.61
10	BP Bellow Side	$Braze$	195	0.74
13	Power Coupler Port	$Braze$	223.8	0.85
12	Vacuum Port	$Braze$	224.75	0.85
14	Transition Ring SS316L	$Braze$	361	0.53
16	Donut Rib	EBW	93	0.14
15	Nb Transition Ring	EBW	73.6	0.11

3.1.15 Load Case 2: Cryogenic Temperature (Tuner Load)

- **Loads** - The load combination for this analysis was the following:

$$(P + D + T_1 + T_2) \tag{23}$$

$P = 0.4$ MPa (Helium Pressure) which is the target value for $MAWP_{CT}$
$D =$ (mass of system)·(gravity)
$T_1 = 7500\ N$
$T_2 =$ Loads due to thermal contraction

- **Results** - The Principal Membrane + Bending (linearized) stress have been calculated through proper stress characterization lines (SCL) as stated by the ASME Code.

Table 17: Local Failure for Load Case 2 with Tuner Load

Weld Number Figure 8	Weld Location	Weld Type	$\sigma_{1L} + \sigma_{2L} + \sigma_{3L}$ [MPa]	η
7	BP Bellow Side	TIG	335.28	0.73
2	BP Ring Side	TIG	280.9	0.61
$1i$	Transition Ring Inside	TIG	272.3	0.59
$1o$	Transition Ring Outside	TIG	128.4	0.28
5	Cfr Bellow Side	TIG	27.85	0.06
3	Cfr Transition Ring Side	TIG	18.76	0.04
$6ss$	Longitudinal Support Side (NS)	TIG	90.8	0.02
$6w$	Longitudinal Weld (NS)	TIG	63.04	0.14
8	Vacuum Port	TIG	153.72	0.34
4	Power Coupler Port	TIG	134.1	0.29
11	BP Ring Side	$Braze$	527.9	0.63
10	BP Bellow Side	$Braze$	540.43	0.67
13	Power Coupler Port	$Braze$	218.55	0.83
12	Vacuum Port	$Braze$	220.52	0.84
14	Transition Ring SS316L	$Braze$	330	0.48
16	Donut Rib	EBW	94.32	0.14
15	Nb Transition Ring	EBW	74	0.11

3.2 Tuner

3.2.1 Support Arm Only

The loads applied in the Support Arm Only analysis, as seen in Figure 16, were the following:

- $F_{motor} = 625\,N$ (Force from coarse motor applied near pins)
- F_{grav} = -(gravity)(mass of system)
- Fixed Support - Support given to mathematical model (Purple face)

The stiffness and stress values calculated for the Support Arm Only analysis were the following:

- Stiffness: $k = 114,160\,\frac{N}{mm}$
- Max Stress: $\sigma_{max} = 10.6\,MPa$

The figures shown here below give mesh, deflection, load, and stress views of the support arm during the analysis.

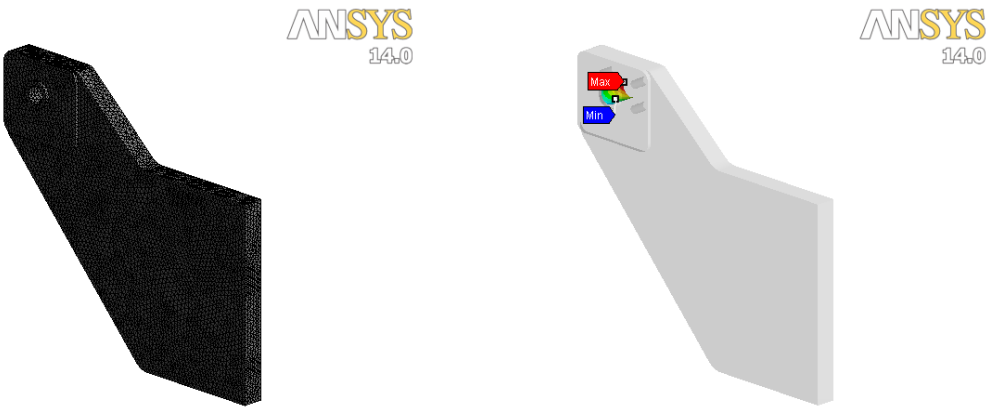

Figure 15: Shown above are views of both the mesh used in the support arms stiffness analysis (left) and the calculated deflection (right).

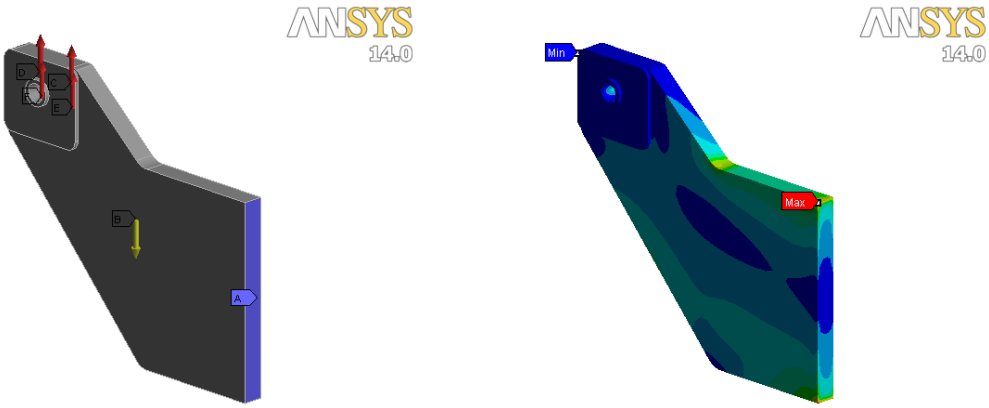

Figure 16: Shown here are views of the applied loads in the mathematical model (left) and the stress concentration for the support arms analysis (right).

3.2.2 Support Arm and Motor Connection

The loads applied in the Support Arm and Motor Connection analysis, as seen in Figure 18, were the following:

- $F_{motor} = 1250\ N$ (Force from coarse motor applied on motor casing)
- F_{grav} = -(gravity)(mass of system)
- Fixed Support - Support given to mathematical model (Purple face)

The stiffness and stress values calculated for the Support Arm and Motor Connection analysis were the following:

- Stiffness: $k = 133,910 \frac{N}{mm}$
- Max Stress: $\sigma_{max} = 35.37\, MPa$

The figures shown here below give mesh, deflection, load, and stress views of the support arm and motor connections during the analysis.

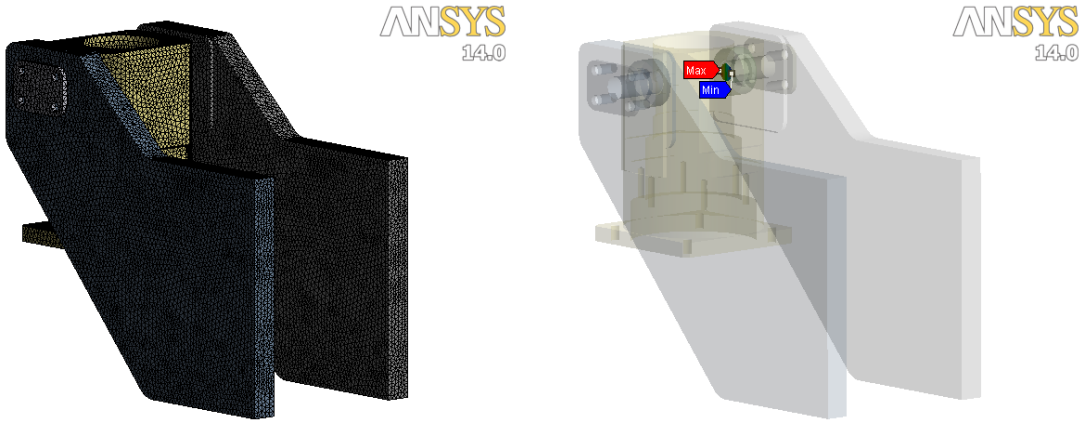

Figure 17: Shown above are views of both the mesh used in the (support + coarse motor connection) stiffness analysis (left) and the calculated deflection (right).

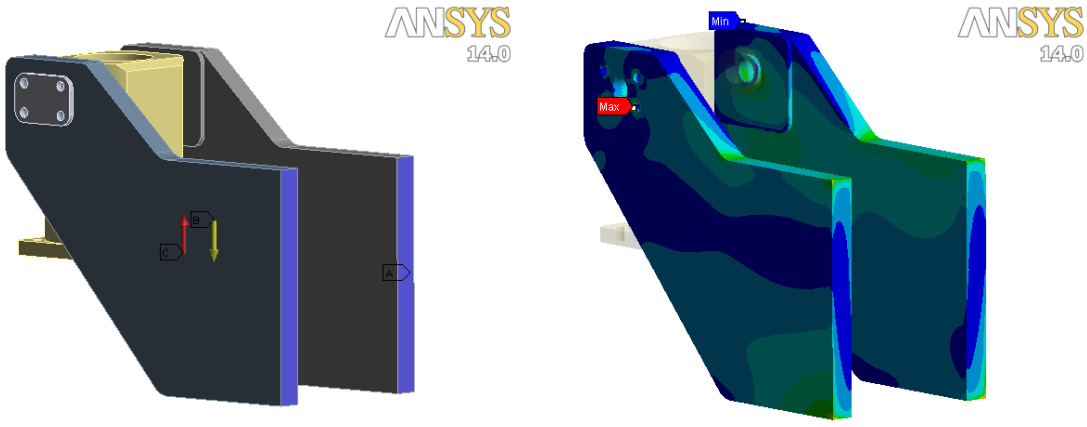

Figure 18: Shown here are views of the applied loads in the mathematical model (left) and the stress concentration for the support arms plus motor connections analysis (right).

3.2.3 Support and SSR1 Resonator

The loads applied in the Support and SSR1 Resonator analysis, as seen in Figure 20, were the following:

- $F_{motor} = 1250\, N$ (Force from coarse motor applied on motor casing)
- F_{grav} = -(gravity)(mass of system)

- $F_{plate} = (2) \cdot 1250\ N$ (Equilibrium force from coarse motor applied by tuner support welded to top section of the plate [Note: multiplied by two because there are two seperate forces applied in the model])
- $F_{arm} = -7500\ N$ (Equilibrium force from coarse motor applied by tuner arm deflection probes near the beam pipe of the pressure vessels)
- $F_{hv} = 3750\,N$ (Equilibrium force from coarse motor applied by second tuner arm connection to helium vessel on the opposite side of the support arms)
- Fixed Support - Support given to mathematical model (Purple face)

The stiffness and stress values calculated for the Support and SSR1 Resonator analysis were the following:

- Stiffness: $k \approx 100,775\ \frac{N}{mm}$
- Max Stress: $\sigma_{max} = 159\ MPa$

The figures shown here below give mesh, deflection, load, and stress views of the support and SSR1 resonator during the analysis.

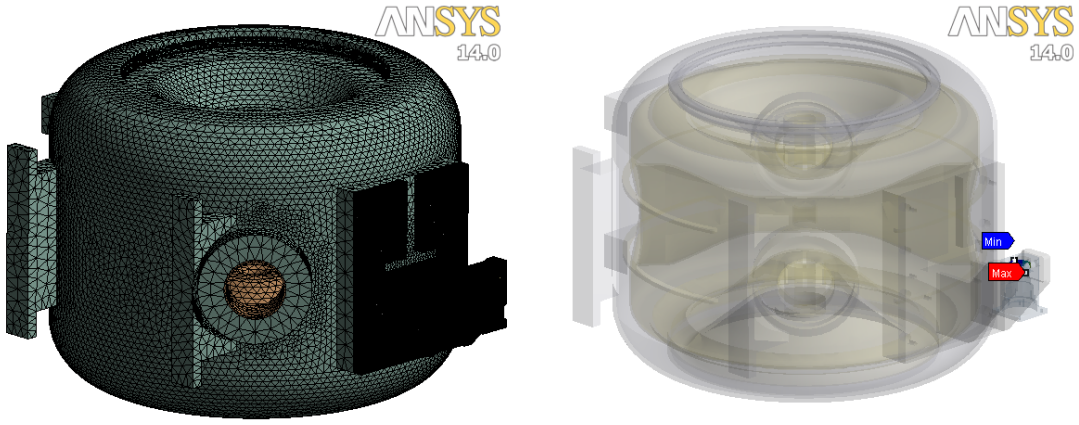

Figure 19: Shown above are views of both the mesh used in the "true" stiffness analysis (left) and the calculated deflection (right).

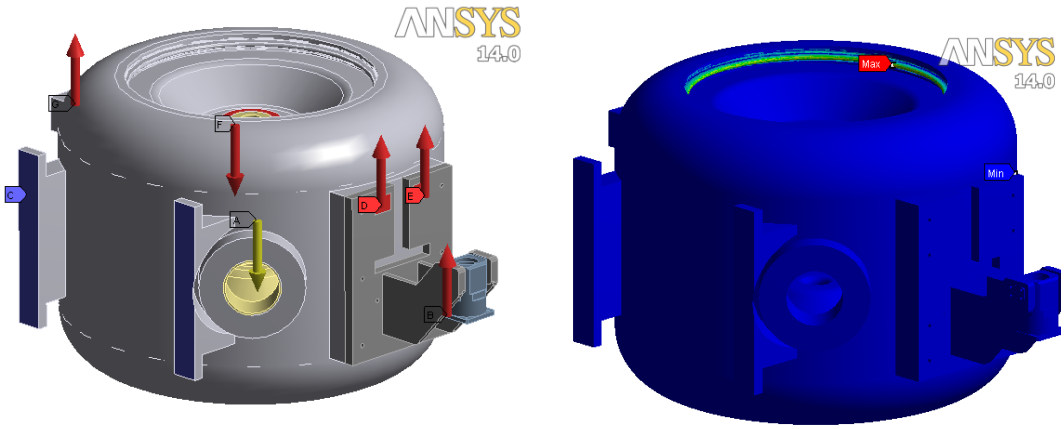

Figure 20: Shown above are views of both the applied loads used in the mathematical model (left) and the calculated stress concentration in the "true" stiffness analysis (right).

4 Disscussion

4.1 Pressure Vessels

The results obtained by all of the numerical analyses performed for the pressure vessels of the SSR1 resonator met the design requirements set forth by the ASME BPV Code. As listed in section 2, the failure modes that must be satisfied are, Protection Against Plastic Collapse, Protection Against Collapse from Buckling, Protection Against Failure from Cyclic Loading, and Protection Against Local Failure.

- Using the final pressure convergence, the results of the plastic collapse, global criterion 1, room temperature analysis, satisfied the criteria set forth by the ASME BVP Code. The analysis, after a considerable amount of running time, was stopped due to non-convergence. Hence, the analysis at room temperature using The University of Pisa test results show the system safely operating until a final pressure. The pressures above this final pressure lead to non-convergence and therefore, system failure. The elastic-plastic analysis shows that the plastic failure occurs in the cavity at the end-wall (bellows side) area where it is connected to the daisy ribs. The $MAWP$ for room temperature obtained by the analysis must be greater than $0.2\,MPa$. As stated in section 3.1.2 the calculated $MAWP$ was $0.280\,MPa$, therefore the pressure vessels of the SSR1 resonator meet the requirements for the ASME Code's Protection Against Plastic Collapse.

- The results of the plastic collapse, global criterion 2, cryogenic temperature analysis, satisfied the criteria set forth by the ASME BVP Code. The $MAWP$ for cryogenic temperature obtained by the analysis must be greater than $0.4\,MPa$. As stated in section 3.1.3 the calculated $MAWP$ was $0.897\,MPa$, therefore the pressure vessels of the SSR1 resonator meet the requirements for the ASME Code's Protection Against Plastic Collapse.

- Using the final pressure convergence, the results of the plastic collapse, global criterion 2, room temperature analysis, satisfied the criteria set forth by the ASME BVP Code. The $MAWP$ for room temperature obtained by the analysis must be greater than $0.2\,MPa$. As stated in section 3.1.4 the calculated $MAWP$ was $0.278\,MPa$, therefore the pressure vessels of the SSR1 resonator meet the requirements for the ASME Code's Protection Against Plastic Collapse.

- The results of the buckling, type 1, room temperature analysis, satisfied the criteria set forth by the ASME BVP Code. The first element to buckle was the niobium cavity and buckling occurred at a

pressure of 3.309 MPa. In Part 5 of the ASME Code, 5.4.1.2 provides a design factor discussed in the Type 1 paragraph of section 2.1. Also given in Paragraph 5.4.1.3 is a capacity reduction factor of $\beta_{cr} = 0.8$ for unstiffened and ring stiffened cylinders and cones under external pressure. Using this capacity reduction value it was found that the minimum design factor is, $\Phi_B = 2.5$. The $MAWP$ for room temperature obtained by the analysis must be greater than 0.2 MPa. As stated in section 3.1.6 the calculated $MAWP$ was 1.324 MPa, therefore the pressure vessels of the SSR1 resonator meet the requirements for the ASME Code's Protection Against Failure from Buckling.

- The results of the buckling, type 1, cryogenic temperature analysis, satisfied the criteria set forth by the ASME BVP Code. The first element to buckle was the cavity and buckling occurs at a pressure of 2.793 bar. In Part 5 of the ASME BPV Code, 5.4.1.2 provides a design factor discussed in the Type 1 paragraph of section 2.1. Also given in Paragraph 5.4.1.3 is a capacity reduction factor of $\beta_{cr} = 0.8$ for unstiffened and ring stiffened cylinders and cones under external pressure. Using this capacity reduction value it was found that the minimum design factor is, $\Phi_B = 2.5$. The $MAWP$ for cryogenic temperature obtained by the analysis must be greater than 0.4 MPa. As stated in section 3.1.6 the calculated $MAWP$ was 1.117 MPa, therefore the pressure vessels of the SSR1 resonator meet the requirements for the ASME Code's Protection Against Failure from Buckling.

- The results of the cyclic loading analysis, which can be seen in section 3.1.8, satisfied the criteria set forth by the ASME BVP Code. There was no plastic deformation in the overall dimensions of the SSR1 resonator, therefore the pressure vessels of the SSR1 resonator meet the requirements for the ASME Code's Protection Against Failure from Cyclic Loading.

- The results of the local failure, room temperature (NO Tuner Load) analysis, section 3.1.12, satisfied the criteria set forth by the ASME BVP Code. It can be seen in Table 14 that all of the weld location ratio's between the summation of principal stresses and $4S$ are less than the allowable limit. The closest approach to the allowable stress limit occurred at the Beam Pipe Bellow Side brazed joint, which reaches 0.54 of the allowable stress limit. Meaning that the Beam Pipe - Bellow Side - brazed joint is the weakest element of the SSR1 resonator for this load combination. The Beam Pipe located on the bellow side also has the highest stresses among the TIG welds. However, the stresses generated in the SSR1 resonator are below the allowed limit and therefore satisfy the local failure criteria. Figure 21 below shows the results of the maximum principal stress distribution at each weld location for load case 1 at room temperature:

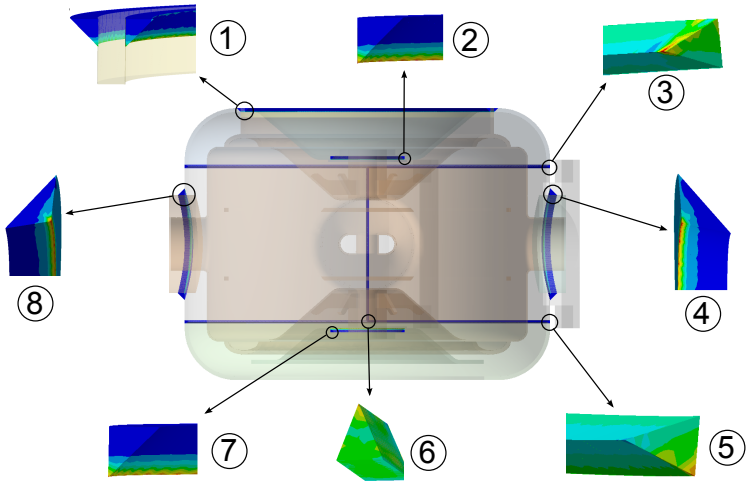

Figure 21: Shown here above are eight different weld locations on the SSR1 resonator and an element of the maximum principal stress evaluation for load case 1 at RT.

- The results of the local failure, room temperature (Tuner Load) analysis, section 3.1.13, satisfied the criteria set forth by the ASME BVP Code. It can be seen in Table 15 that all of the weld location ratio's between the summation of principal stresses and $4S$ are less than the allowable limit. The closest approach to the allowable stress limit occurred at the Beam Pipe - Bellow Side TIG weld, which reaches 0.39 of the allowable stress limit. Meaning that the Beam Pipe - Bellow Side TIG weld is the weakest element of the SSR1 resonator for this load combination. The Beam Pipe located on the bellow side also has the highest stresses among the brazed joints. However, the stresses generated in the SSR1 resonator are below the allowed limit and therefore satisfy the local failure criteria.
- The results of the local failure, cryogenic temperature (NO Tuner Load) analysis, section 3.1.14, satisfied the criteria set forth by the ASME BVP Code. It can be seen in Table 16 that all of the weld location ratio's between the summation of principal stresses and $4S$ are less than the allowable limit. The closest approach to the allowable stress limit occurred in both the Vacuum Port and Power Coupler Port brazed joint, which reaches 0.85 of the allowable stress limit. Meaning that both the Vacuum Port and Power Coupler Port brazed joint are the weakest elements of the SSR1 resonator for this load combination. However, the stresses generated in the SSR1 resonator are below the allowed limit and therefore satisfy the local failure criteria.
- The results of the local failure, cryogenic temperature (Tuner Load) analysis, section 3.1.15, satisfied the criteria set forth by the ASME BVP Code. It can be seen in Table 17 that all of the weld location ratio's between the summation of principal stresses and $4S$ are less than the allowable limit. The closest approach to the allowable stress limit occurred in the Vacuum Port brazed joint, which reaches 0.84 of the allowable stress limit. Meaning that the Vacuum Port brazed joint is the weakest element of the SSR1 resonator for this load combination. However, the stresses generated in the SSR1 resonator are below the allowed limit and therefore satisfy the local failure criteria.

4.2 Tuner

For the first support arm analysis, which included one support arm only in the mathematical model, it was important to ensure that the stiffness calculated from this test met the requirements. This analysis was the simplest of the three performed. There was only one force and one fixed support applied in the mathematical model. The applied loads can be seen in Figure 16. A mesh of $2\,mm$, which can be seen in Figure 15, was used on the support arm for the FEA model. The calculated deflection values and stress concentrations can be seen in Figure 15. The calculated deflection for the support arm was $\delta = 0.005474\,mm$. This deflection gave a stiffness value of $k = 114,160\,\frac{N}{mm}$. The maximum stress value that was calculated occurred at the top of the weld connecting the support arm to the plate and equalled $10.6\,MPa$. Therefore, the support arm alone has met the design requirements and the next phase of analysis was to add the coarse motor connections to the mathematical model.

For the second analysis, which included both support arms as well as the coarse motor casing and it's connections, the stiffness was expected to stay the same or raise slightly. This results from two variables; first, the added motor casing will connect the support arms in such a way as to raise the stiffness of the support system. Second, with the added connections comes the added difficulty to properly mathematically model the system and therefore approximations were made. The added connections included the bearings and pins. The housing characteristics of the bearing in the coarse motor casing was found difficult to simulate properly and therefore was an approximation of this analysis. There were other approximations made in the analysis but the approximations overall were kept to a minimum. Since both support arms were introduced in this analysis there was two fixed supports applied. Also for the same reason the applied force was doubled. The applied loads of this analysis can be seen in Figure 18. The mesh size used in this analysis was also $2\,mm$. The calculated deflection values and stress concentrations can be seen in Figure 17. The calculated deflection for the (support arm + coarse motor connection) was $\delta = 0.009334\,mm$. This deflection gave a stiffness value of $k = 133,910\,\frac{N}{mm}$. The maximum stress value occurred near the coarse motor pin locations and had a value of $35.37\,MPa$. Therefore, the support arm and coarse motor connections has met the design requirements and the next phase of analysis was to add the SSR1 resonator to the mathematical model.

For the final analysis, which included the support arms system and the pressure vessels of the SSR1 resonator, the stiffness was expected to be slightly less than the second analysis and closer to the stiffness value of the first analysis. The main variable responsible for the decrease in stiffness is the helium vessel of the SSR1 resonator. This vessel has a thin, 6 mm shell which offers little support for the plate. This analysis was by far the most complex of the three and gave the "true" stiffness. All of the components from the previous analysis plus the support plate, the helium vessel, and the niobium cavity were included in this analysis. Again, there were several approximations that needed to be made when creating the mathematical model. The main approximations were the Spot Welds for screws and the use of a Planar Joint to create a contact between the plate and helium vessel. This rigid Planar contact did not allow the plate to deform as it normally would and therefore a separate analysis concerning the plate was made. In this analysis the plate was given a no Planar support so that the plate deformed without constraint. The areas where the plate penetrated the helium vessel where then made into imprinted faces. In the approximated analysis these imprinted faces where then made the new Planar Joint and the analysis was re-run. The surface area of plat-to-helium vessel that is fixed was significantly reduced allowing a more realistic deformation to occur. Due to the addition of the helium vessel the fixed support load changed to the support components of the helium vessel. Also, because of the entire system being present in this model the addition of equilibrium forces were necessary. The force applied on the support arms comes from the motor which is held in place by the helium vessel, therefore creating an internal force. To give a correct mathematical model the support force must be countered by equilibrium forces of proper magnitude placed at the tuner system's contact points. The applied loads of this analysis can be seen in Figure 20. The mesh size used for the components of the previous analysis remained 2 mm but the added components had an element size of 8 mm. The calculated deflection values and stress concentrations can be seen in Figure 19. The calculated deflection for the (support + SSR1 resonator) was $\delta \approx 0.0124\, mm$. This deflection gave a stiffness value of $k \approx 100,775\, \frac{N}{mm}$. The maximum stress value that was calculated 159 MPa. The deflection that was calculated during the final analysis gave a final deflection that was within 1% of the target value given for the support arms. This analysis has been worked on to try and make the behavior of the support as realistic as possible but the results remain an approximation. As stated in section 2.2 the REQUIRED stiffness value was $70,000\, \frac{N}{mm}$ and the $100,000\, \frac{N}{mm}$ target value was for safety. The calculated value for the final analysis surpassed this requirement by 30.5%. This support design has a stiffness above the required value and also above, but very close to, the target value for the "true" stiffness. Therefore, the support arms component has met the design requirements.

With all of the ASME BPV Section VIII, Division 2, Part 5 design requirements for the pressure vessels of the SSR1 resonator successfully met the design of the SSR1 resonator is a qualified component design. There are still several additions that need to be made to the Engineering Note for the Dressed SSR1 Cavities. The structure of the Note has been set but images and tables are being gathered and are being assigned placements in the Engineering Note. The next steps that follow these analyses are to get drawings that represent the pressure vessels of the SSR1 resonator developed. The drawings provide a manufacturer precise dimensions and instructions on how to construct the pressure vessels. Also, the tuner system, which attaches to the pressure vessels, is under design changes and will be going through further analyses. The further analyses will be to review the work that has been done recently and to and to also perform analyses on sections of the tuner that have yet to be analyzed.

5 Acknowledgements

I want to thank Fermilab and the U.S Department of Energy, Office of Science for developing and funding the Summer Internships for Science and Technology (SIST) program and allowing me the opportunity to participate during the summer of 2012. I would also like to thank the committee members of the SIST program for all the hard work they put forth while organizing such a great program.

I would finally like to give a much-deserved thanks to Donato Passarelli, Margherita Merio, and Leonardo Ristori for, most importantly, being very helpful towards me through my internship and also for making my experience at Fermilab a great one.

6 Appendices and Nomenclature

6.1 Nomenclature

α - Coefficient of Thermal Contraction
BP - Beam Pipe
Cfr - Circumferential
CT - Cryogenic Temperature
E - Modulus of elasticity evaluated at the temperature of interest, see Annex 3.E
ε_p - Stress-strain curve fitting parameter
m_2 - Curve fitting exponent for the stress-strain curve equal to the true strain at the true ultimate stress
$MAWP$ - Maximum Allowable Working Pressure
ν - Poisson's Ratio
R - Engineering yield to engineering tensile ratio
RT - Room Temperature
S Allowable stress based on the material of construction and design temperature
σ_1 - Principal stress in the 1-direction
σ_2 - Principal stress in the 2-direction
σ_3 - Principal stress in the 3-direction
σ_{uts} - Engineering ultimate tensile stress evaluated at the temperature of interest, see paragraph 3.D.2
T - Temperature
Y_s - Yield Strength
Y_{ut} - Engineering Ultimate Strength

6.2 Reference Tables

5.14 Tables

Table 5.1 – Loads And Load Cases To Be Considered In A Design

Loading Condition	Design Loads
Pressure Testing	1. Dead load of component plus insulation, fireproofing, installed internals, platforms and other equipment supported from the component in the installed position. 2. Piping loads including pressure thrust 3. Applicable live loads excluding vibration and maintenance live loads. 4. Pressure and fluid loads (water) for testing and flushing equipment and piping unless a pneumatic test is specified. 5. Wind loads
Normal Operation	1. Dead load of component plus insulation, refractory, fireproofing, installed internals, catalyst, packing, platforms and other equipment supported from the component in the installed position. 2. Piping loads including pressure thrust 3. Applicable live loads. 4. Pressure and fluid loading during normal operation. 5. Thermal loads.
Normal Operation plus Occasional (note: occasional loads are usually governed by wind and earthquake; however, other load types such as snow and ice loads may govern, see ASCE-7)	1. Dead load of component plus insulation, refractory, fireproofing, installed internals, catalyst, packing, platforms and other equipment supported from the component in the installed position. 2. Piping loads including pressure thrust 3. Applicable live loads. 4. Pressure and fluid loading during normal operation. 5. Thermal loads. 6. Wind, earthquake or other occasional loads, whichever is greater. 7. Loads due to wave action
Abnormal or Start-up Operation plus Occasional (see note above)	1. Dead load of component plus insulation, refractory, fireproofing, installed internals, catalyst, packing, platforms and other equipment supported from the component in the installed position. 2. Piping loads including pressure thrust 3. Applicable live loads. 4. Pressure and fluid loading associated with the abnormal or start-up conditions. 5. Thermal loads. 6. Wind loads.

Figure 22: Table 5.1

Table 5.8 – Temperature Factors For Fatigue Screening Criteria

Metal temperature Differential		Temperature Factor For Fatigue Screening Criteria
°C	°F	
28 or less	50 or less	0
29 to 56	51 to 100	1
57 to 83	101 to 150	2
84 to 139	151 to 250	4
140 to 194	251 to 350	8
195 to 250	351 to 450	12
Greater than 250	Greater than 450	20

Notes:

1. If the weld metal temperature differential is unknown or cannot be established, a value of 20 shall be used.
2. As an example illustrating the use of this table, consider a component subject to metal temperature differentials for the following number of thermal cycles.

Temperature Differential	Temperature Factor Based On Temperature Differential	Number Of Thermal Cycles
28 °C (50 °F)	0	1000
50 °C (90 °F)	1	250
222 °C (400 °F)	12	5

The effective number of thermal cycles due to changes in metal temperature is:

$$N_{\Delta TE} = 1000(0) + 250(1) + 5(12) = 310 \; cycles$$

Figure 23: Table 5.8

Table 5.9 – Fatigue Screening Criteria For Method A

Description		
Integral Construction	Attachments and nozzles in the knuckle region of formed heads	$N_{\Delta FP} + N_{\Delta PO} + N_{\Delta TE} + N_{\Delta T\alpha} \leq 350$
	All other components that do not contain a flaw	$N_{\Delta FP} + N_{\Delta PO} + N_{\Delta TE} + N_{\Delta T\alpha} \leq 1000$
Non-integral construction	Attachments and nozzles in the knuckle region of formed heads	$N_{\Delta FP} + N_{\Delta PO} + N_{\Delta TE} + N_{\Delta T\alpha} \leq 60$
	All other components that do not contain a flaw	$N_{\Delta FP} + N_{\Delta PO} + N_{\Delta TE} + N_{\Delta T\alpha} \leq 400$

Figure 24: Table 5.9

References

[1] T. Nicol, S. Cheban, M. Chen, S. Kazakov, F. McConologue, Y. Orlov, L. Ristori, D. Passarelli, I. Terechkine, V. Poloubotko, O. Pronitchev. *SSR1 Cryomodule Design for PXIE*, 2012.

[2] L. Ristori, M. H. Awida, I. Gonin, M. Merio, D. Passarelli, V. Yakovlev. *Design of SSR1 Spoke Resonators for PXIE*, 2012.

[3] Wands, Bob, *A stress Analysis of the SSR1 SRF Cavity According to the Rules of the 2007 ASME Boiler and Pressure Vessel Code's Section VIII, Div. 2, Part 5.* 2009

[4] Page, Thomas M., *Analysis of HTS Lead HX Braze Boint.* 2009

[5] National Bureau - Cryogenic Division, *Handbook on Material for Superconducting Machinery.* 1974

[6] Wood, Dr. Jim, *Intoduction to PV - Design by Analysis* http://personal.strath.ac.uk/j.wood/CCOPPS_DBA/Notes/dba_intro_content_1.htm

[7] Ristori, Leonardo; Toter, W., *Development at ANL of a Copper-Brazed Joint for the Coupling of the Niobium Cavity End Wall to the Stainless Steel Helium Vessel in the Fermilab SSR1 resonator.*

[8] Merio, Margherita, *Material Properties for Engineering Analyses of SRF Cavities.* 2011.

[9] Fuerst, J.D.; Toter, W.F.; Shepard, K.W., *Niobium to Stainless Steel Braze Transition Development*